Efficiency Enhancement and Optical Guiding in a Tapered High-Power Finite-Pulse Free-Electron Laser

B. Hafizi,[a] A. Ting, P. Sprangle, and C. M. Tang
Beam Physics Branch, Plasma Physics Division, Naval Research Laboratory, Washington, D.C. 20375-5000
(Received 13 July 1989)

We compare the radiation output from simulations of a finite-pulse high-power laser for several tapering rates. A fast taper leads to a tenfold increase in efficiency as compared to a slow taper, with little change in peak radiation intensity. The enhanced power for fast tapering rates is due to an increase in the optical-pulse cross section, brought about by a reduction in refractive guiding. This is analyzed by an envelope equation for the radiation beam. For the tapering rates leading to the highest powers, the optical pulse is virtually free of sideband modulation.

PACS numbers: 42.55.Tb, 52.75.Ms

One-dimensional free-electron-laser (FEL) theory predicts that the radiation intensity increases when the wiggler is tapered, leading to higher efficiency.[1-3] Thus, one would expect that a faster taper should lead to a higher output intensity and efficiency. Multidimensional results[4] are generally reported as an increase in output power, without specifying the intensity, which is a key parameter in many applications. We have studied a high-power, finite-pulse FEL with a 3D, axisymmetric, time-dependent code. Comparison of the radiation at the wiggler exit for several tapering rates confirms the *increase* in power enhancement with faster tapering rates. Surprisingly, this improvement is not primarily due to an increase in the peak intensity within the pulse; rather, it is due to an increase in the radiation spot size. It turns out that the extra energy extracted from the electron beam is spread over a larger cross section due to a reduction in optical guiding.

Two causes of guiding,[1-3,5-11] gain focusing and refractive guiding, have been distinguished based on the notion of a complex refractive index.[8] In general, these two participate simultaneously and their combined effect on the spot size can be ascertained via the envelope equation for the radiation beam in an FEL.[10] We find that refractive guiding, which dominates gain focusing, diminishes as the tapering rate is increased. As a result the wave fronts become more convex and the spot size increases.

To examine guiding, consider the FEL refractive index[1-3,5-10]

$$\mu = 1 + (\omega_b/\omega)^2 (a_w/2|a|)\langle \exp(-i\xi)/\gamma \rangle ,$$

where ω_b is the plasma frequency, and $a_w = |e| B_w/k_w mc^2$ and $a = |e| A/mc^2$ are the normalized vector potentials of the wiggler and radiation fields, with $-|e|$ the charge and m the mass of an electron with energy γmc^2, B_w the amplitude, and $2\pi/k_w$ the period of the wiggler. The electron phase relative to the ponderomotive potential is ξ, and $\langle \cdots \rangle$ denotes a beam average. The optical vector potential is represented by $Ae^{i\omega(z/c-t)}\hat{\mathbf{e}}_x/2 + \text{c.c.}$, where $A(\mathbf{r},t)$ is a slowly varying amplitude, ω is the frequency, and $\hat{\mathbf{e}}_x$ is the unit vector along the x axis. The real part of μ governs the refractive effect and the imaginary part describes the gain. Their combined role in the evolution of the radiation spot size $r_s(z,t)$ is expressed by the envelope equation[10]

$$r_s'' + K^2(z,t,r_s,|a_0|) r_s = 0 ,$$

$$K^2 \equiv (2c/\omega)^2 [-1 + 2C\cos\xi_r + C^2 \sin^2\xi_r + (\omega/2c) r_s^2 C' \sin\xi_r] r_s^{-4} ,$$

where a_0 is the amplitude of the fundamental Gaussian mode, $C = (2I_b/17\gamma_r) H a_w/|a_0|$, the prime symbol $\equiv \partial/\partial z + c^{-1}\partial/\partial t$, I_b is the beam current in kiloamperes, H, which is a form factor related to the transverse profile of the electron beam, is roughly a constant and close to unity herein, γ_r is the relativistic factor for a resonant electron, and ξ_r is the resonance phase approximation for $\langle \xi \rangle$. The -1 in the expression for K^2 is due to vacuum diffraction, $2C\cos\xi_r$ contributes to refractive guiding arising from the real part of μ, and the third and fourth terms, due to the imaginary part of μ, contribute to gain focusing. The relative importance of these will be discussed along with the simulation results.

The code employs the method of source-dependent expansion,[10] using Gaussian Laguerre functions to evolve the optical field.[12] Betatron motion in a wiggler with parabolic pole faces is included. The initial electron distribution is a parabolic along the axial direction and in the transverse plane. The parameters for the computations, which are similar to those for the proposed rf-linac FEL experiment at the Boeing Aerospace Company, are listed in Table I.[11] The input power is sufficient to initially trap all the electrons. The tapering of the wiggler field, commencing at the entrance, is obtained by prescribing a constant rate of decrease of electron energy $d\gamma_r/dz < 0$.

For brevity, the results for only two tapering rates will be discussed. Case (a), $-d\gamma_r/dz = 0.1\ \text{m}^{-1}$ ($\xi_r \simeq 1.8°$), has a slow taper, and case (b), $-d\gamma_r/dz = 1.3\ \text{m}^{-1}$

TABLE I. Parameters for a high-power, rf-linac FEL.

Energy γmc^2	175 MeV
Current I_b	450 A
Normalized edge emittance	153 mm mrad
E-beam radius	1 mm
E-beam pulse length	6.7 ps
Wiggler field B_w	6.4 kG
Wiggler period $2\pi/k_w$	4.7 cm
Wiggler length L	42 m
Radiation wavelength $2\pi c/\omega$	1 μm
Initial spot size r_s	1.25 mm
Peak radiation input power	450 MW

($\xi_r \simeq 18°$), has a fast taper. Figure 1 shows the profiles of the optical pulse $|a(z,r=0)|$ and the electron pulse at the end of the wiggler for cases (a) and (b). Note that the *peak* intensity ($\sim |a|^2$) is about the same in both cases. The asymmetry of the optical pulse is due to the slippage of the electrons, which causes a greater amplification of the trailing side of the optical pulse as compared to the leading edge. Taking account of the finite transverse extent of the pulse, the slippage over a wiggler of length L is

$$\tfrac{1}{2} L[(1+a_w^2/2)/\gamma_r^2 - (\pi c/\omega r_s)^2] \simeq 1 \text{ mm},$$

where the second term is due to transverse effects. This is comparable to that observed in Fig. 1. Figure 1(a) also illustrates the growth of sideband modulations from the leading to the trailing edge of the optical pulse. Note the sharp reduction in the modulation of the pulse in the more rapidly tapered case (b), Fig. 1(b), as in a recent experiment.[13]

Figure 2 shows the radiation spot size $r_s(z)$ (solid line) and wave-front curvature $\alpha(z)$ (dashed line), with $\alpha(z)$ normalized to $\omega r_s^2/2c$. Note that in the region where the field amplitude is significant the spot size is much smaller than in the surrounding regions where $a \simeq 0$, and r_s and α evolve as in *vacuum*. Note further that for case (a), shown in Fig. 2(a), $\alpha \simeq 0$ within pulse, indicating roughly planar wave fronts. On the other hand, for case (b), shown in Fig. 2(b), $\alpha > 0$, indicating that the wave fronts are convex everywhere.

Figures 3 and 4 show the real and imaginary parts of $\mu(z)$ at the end of the wiggler. Comparing Figs. 3(a) and 3(b) it is apparent that Reμ is significantly larger in the former, case (a). On the other hand, noting that Im$\mu < 0$ corresponds to gain, Fig. 4(a) indicates that the net gain is approximately zero after averaging over the synchrotron modulations, whereas the more rapidly tapered case (b) of Fig. 4(b) is seen to have a net gain in the region where the optical field is significant.

The implication of these results with regard to the spot size may be ascertained by a consideration of the terms in K^2 in the envelope equation. Taking account of the fraction of trapped electrons, one finds that in going from case (a) to case (b) the gain-focusing term

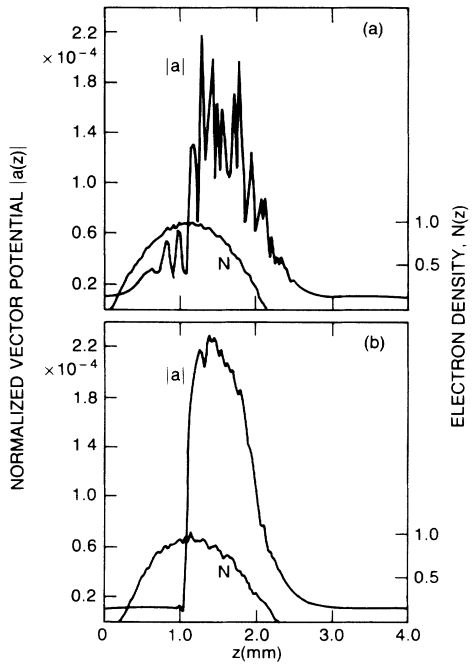

FIG. 1. Vector potential $|a(z,r=0)|$ and linear electron density $N(z)$ at wiggler exit. (a) Slow tapering rate, resonance phase $\xi_r \simeq 1.8°$ [case (a)]; (b) rapid tapering rate, resonance phase $\xi_r \simeq 18°$ [case (b)]. Note that intensity $\propto |a|^2$.

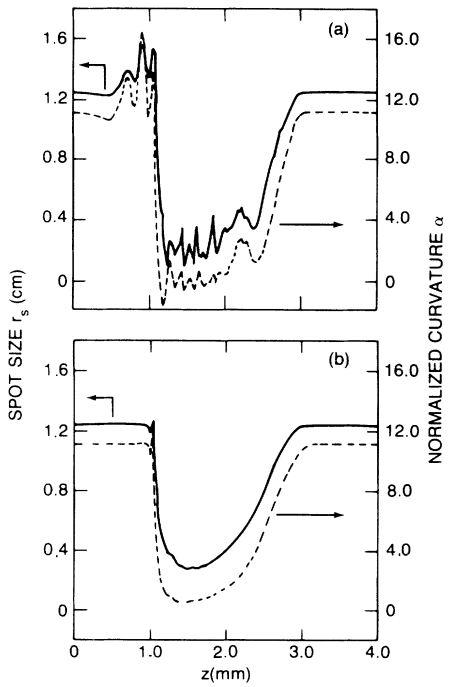

FIG. 2. Spot size $r_s(z)$ and normalized curvature $\alpha(z)$ at wiggler exit. (a) Slow taper [case (a)]; (b) rapid taper [case (b)].

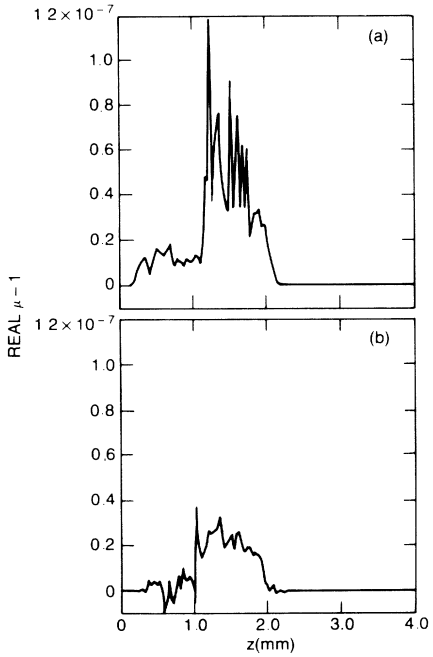

FIG. 3. Real $\mu(z,r=0)$ part of refractive index at wiggler exit. (a) Slow taper [case (a)]; (b) rapid taper [case (b)].

$C^2\sin^2\xi_r$ increases from 2.4×10^{-3} to 7×10^{-2}. The other term, $(\omega/2c)r_s^2C'\sin\xi_r$, changes from -4.4×10^{-3} to -2.4×10^{-2}, the negative sign indicating a defocusing contribution. On the other hand, the refractive-guiding term $2C\cos\xi_r$ decreases from 3.1 to 1.6. The increase in the magnitude of the gain-focusing terms in going from case (a) to case (b) is principally due to the increase in ξ_r. Concurrently, the 50% reduction in the refractive-guiding term is due to the increase in $|a_0|$ and the decrease in a_w. Since the refractive-guiding term is the dominant term, the reduction in its value leads to a decrease in K^2, and hence to reduced optical guiding. The net effect is the increase in the spot size and the curvature observed in Fig. 2(b) as compared to Fig. 2(a). In other words, the wave fronts become increasingly convex with faster tapering rate.

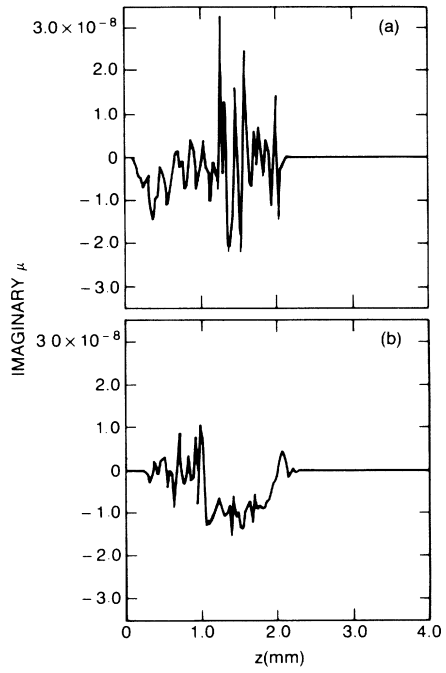

FIG. 4. Imaginary $\mu(z,r=0)$ part of refractive index at wiggler exit. (a) Slow taper [case (a)]; (b) rapid taper [case (b)].

Figure 5 summarizes the results for the nine tapering rates $-d\gamma_r/dz=0.1,0.3,\ldots,1.7\ \mathrm{m}^{-1}$, corresponding to $\xi_r\simeq1.8°,3.5°,\ldots,35°$. Beyond $-d\gamma_r/dz=0.3\ \mathrm{m}^{-1}$, the amplitude $|a|$ is fairly constant up to $-d\gamma_r/dz=1.3\ \mathrm{m}^{-1}$, after which it decreases. However, there is a near-monotonic increase in the spot size. Therefore, it is the increased transverse extent of the optical field—and not an increase in intensity—that is responsible for the enhancement in the power ($\propto|r_sa|^2$) observed in Fig. 5. Based on the desired output power and the constraint on the maximum spot size one can determine the optimal

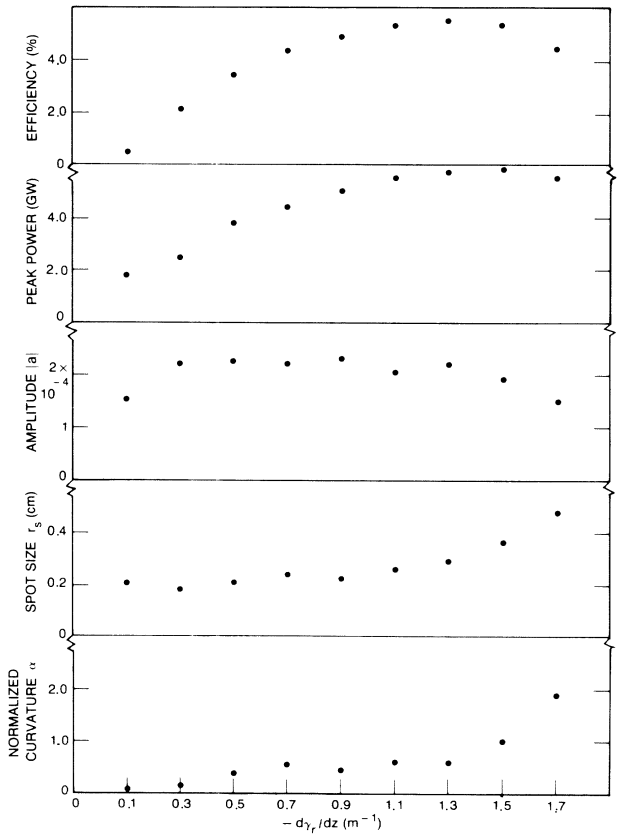

FIG. 5. Summary of results for various tapering rates $-d\gamma_r/dz$. Efficiencies are obtained from total energy in optical field. For other quantities, ordinate values correspond to peak-power point along the pulse, which varies somewhat between the different tapering rates.

tapering from Fig. 5.

Returning to Fig. 1, the period of the sideband modulation in Fig. 1 is within 10% of that given by theory.[14,15] Tapering reduces sideband modulation by decreasing the trapping fraction and by distorting the synchrotron motion.[12,16] The trapping fraction drops from $\sim 40\%$ in case (a) to $\sim 35\%$ in case (b). A measure of the distortion of electron orbits is given by[12] $R \equiv |c(d\gamma_r/dz)/\langle \Omega(\gamma-\gamma_r)\rangle|$ which is the ratio of the change in energy $c\,d\gamma_r/dz$ due to tapering and the change in energy $\langle \Omega(\gamma-\gamma_r)\rangle$ due to synchrotron motion, where $\Omega \simeq ck_w \times [2a_w|a|/(1+a_w^2)]^{1/2}$ is the synchrotron frequency. For case (a), $R \simeq 1\%$, indicating a slight distortion, whereas for case (b), $R \simeq 25\%$, indicating significant modification of the synchrotron motion and thus, reduced sideband modulation, as is indeed observed in Fig. 1(b).

In summary, we find that tapering does not significantly affect the peak intensity in an FEL. Power enhancement is accomplished by spreading the radiation into a larger cross section due to reduced refractive guiding. It should be remarked that tapering can lead to an increase in the intensity if the spot size is held constant. From the envelope equation it can be shown that this may be achieved by suitable "tapering" of the electron-beam radius. For a tapered FEL with the parameters herein, distortion of electron orbits due to tapering is observed to be a significant cause for the reduction in sideband amplitude.

The authors are grateful to Dr. T. F. Godlove, Dr. I. Haber, Dr. W. P. Marable, and Dr. C. W. Roberson for valuable suggestions. This work was supported by ONR through the National Institute of Standards and Technology.

---

[a]Permanent address: Science Applications Intl. Corp., McLean, VA 22101.

[1]P. Sprangle, C. M. Tang, and W. M. Manheimer, Phys. Rev. Lett. **43**, 1932 (1979); Phys. Rev. A **21**, 302 (1980).

[2]N. M. Kroll, P. L. Morton, and M. N. Rosenbluth, IEEE J. Quantum Electron. **21**, 1436 (1981).

[3]D. Prosnitz, A. Szoke, and V. R. Neil, Phys. Rev. A **24**, 1436 (1981).

[4]E. T. Scharlemann, J. Appl. Phys. **58**, 2154 (1985); R. A. Jong, E. T. Scharlemann, and W. M. Fawley, Nucl. Instrum. Methods Phys. Res., Sect. A **272**, 99 (1988); J. E. La Sala, D. A. G. Deacon, and J. M. J. Madey, Nucl. Instrum. Methods Phys. Res., Sect. A **272**, 141 (1988); C. W. Roberson and P. Sprangle, Phys. Fluids B **1**, 3 (1989).

[5]P. Sprangle and C. M. Tang, Appl. Phys. Lett. **39**, 677 (1981).

[6]J. M. Slater and D. D. Lowenthal, J. Appl. Phys. **52**, 44 (1981).

[7]G. T. Moore, Opt. Commun. **52**, 46 (1984).

[8]E. T. Scharlemann, A. M. Sessler, and J. S. Wurtele, Nucl. Instrum. Methods Phys. Res., Sect. A **239**, 29 (1985); Phys. Rev. Lett. **54**, 1925 (1985).

[9]M. Xie and D. A. G. Deacon, Nucl. Instrum. Methods Phys. Res., Sect. A **250**, 426 (1986).

[10]P. Sprangle, A. Ting, and C. M. Tang, Phys. Rev. Lett. **59**, 202 (1987); Phys. Rev. A **36**, 2773 (1987).

[11]C. M. Tang, P. Sprangle, A. Ting, and B. Hafizi, J. Appl. Phys. **66**, 1549 (1989).

[12]B. Hafizi, A. Ting, P. Sprangle, and C. M. Tang, Phys. Rev. A **38**, 197 (1988).

[13]A. Bhattacharjee, S. Y. Cai, S. P. Chang, J. W. Dodd, and T. C. Marshall, in Proceedings of the Tenth International Free-Electron Laser Conference, Jerusalem, Israel, 29 August–2 September 1988 (to be published).

[14]J. C. Goldstein and W. B. Colson, in *Proceedings of the International Conference on Lasers, New Orleans, LA, 1982,* edited by R. C. Powell (STS, McLean, VA, 1983), p. 218; J. C. Goldstein, B. E. Newman, R. W. Warren, and R. L. Sheffield, Nucl. Instrum. Methods Phys. Res., Sect. A **250**, 4 (1986).

[15]R. C. Davidson and S. Wurtele, Phys. Fluids **30**, 557 (1987).

[16]W. B. Colson, Nucl. Instrum. Methods Phys. Res., Sect. A **250**, 168 (1986).